

Chapter 5

Light Extinction Budget

5.1 Assumptions and Data Analysis Techniques

Throughout this chapter several data analysis techniques will be used repeatedly. These techniques, including calculations of reconstructed scattering and reconstructed extinction and multiple linear regression (MLR) analyses are summarized in this subsection.

5.1.1 Available Data

The data necessary to calculate a light extinction budget for a given site are measurements of light extinction and concentrations of fine and coarse particulate matter. Three of the WHITEX sites had sufficient data for extinction budget calculations. These are Page, Canyonlands, and Hopi Point. The particulate data for each site are discussed in detail in Chapter 3. Each site was equipped with both a transmissometer to measure extinction (b_{ext}) and a nephelometer to measure scattering (b_{scat}). These optical measurements are also discussed in detail in Chapter 3.

5.1.2 Chemical Composition of Particulate Matter

The following assumptions were made about the chemical composition of the fine particulate matter: sulfates are ammonium sulfate ($(NH_4)_2SO_4$), nitrates are ammonium nitrate ($(NH_4)NO_3$), and organics have a mean carbon to hydrogen ratio of 3:4. Since the quantities which were measured by the particulate samplers were SO_4 ion, NO_3 ion, and organic carbon, to account for the mass of associated ions, the following definitions will be used throughout the chapter:

$$sulfates = 1.4 \times [SO_4] \quad (5.1)$$

$$nitrates = 1.3 \times [NO_3] \quad (5.2)$$

$$organics = 1.4 \times [organic\ C] \quad (5.3)$$

$$total\ carbon = 1.4 \times [organic\ C] + [light\ absorbing\ C] \quad (5.4)$$

SO_4 ion concentrations used are always those from the IMPROVE sampler module B which is the teflon filter analysed by ion chromatography. Coarse mass was calculated by subtracting the fine mass from the total mass measured by the SCISAS sampler. This is because there were no IMPROVE coarse mass data available. Discussions about choice of which carbon data to use in the extinction budgets are given in a following section.

Fine mass is 0–2.5 μm diameter. Coarse mass is 2.5–15 μm . All data were averaged to 12-hour time periods beginning at 0800 and 2000 local time each day.

The mass of fine soil is generally calculated from the mass of soil-related elements by

$$\begin{aligned} \text{soil} = & 1.89 \times [Al] + 2.14 \times [Si] + 1.20 \times [K] + \\ & 1.40 \times [Ca] + 1.67 \times [Ti] + 1.36 \times [Fe] \end{aligned} \quad (5.5)$$

where the multipliers include the oxide present. As was discussed in more detail in Chapter 3, the collocated measurements of fine soil elements, aluminum (Al), silicon (Si), potassium (K), calcium (Ca), and titanium (Ti) made by the IMPROVE and SCISAS samplers at Page and Hopi Point did not agree well. Iron (Fe) concentrations from the two samplers, however, were similar. (See Appendix 3D for scatter plots of these data.)

In order to determine whether the SCISAS or IMPROVE soil concentrations should be used, reconstructed mass at Page was calculated by summing sulfates, nitrates, organics, absorbing carbon, and soil, then comparing the sum to measured fine mass. This was done using all IMPROVE data and then using all SCISAS data except that IMPROVE nitrate was used for the SCISAS calculation since SCISAS nitrate is total rather than particulate nitrate. This analysis showed that the fit for the SCISAS data was much tighter than for the IMPROVE data, leading to more confidence in the SCISAS soil concentrations. However, SCISAS data are not available at Canyonlands and are on a different time scale at Hopi Point which means IMPROVE particulate data must be used for the light extinction budgets. Since most of the iron is soil related and the SCISAS and IMPROVE iron concentrations agreed quite well, the relationship between IMPROVE iron and SCISAS soil at Page was determined by finding the best fit between these two variables. Based on this fit, fine soil concentrations for all three sites were estimated by IMPROVE fine iron concentrations to be

$$\text{soil} = 33 \times [Fe] \quad (5.6)$$

5.1.3 Relative Humidity Considerations

It is known that pure ammonium sulfate aerosol will rapidly undergo deliquescence (condensation of water vapor onto the solid particles) at approximately 80% relative humidity (RH). The reverse phase change, when the liquid evaporates from the droplets, occurs more slowly over a much broader range of RH. This is referred to as the hysteresis effect. In the atmosphere, the situation is further complicated by internally mixed aerosols which may go through several stages of growth. The RHs at which these stages occur depend on the mixture, but in general are between 60% and 80%.¹² Since high RH complicates the relationship between particle concentrations and light scattering, some analyses were done for "low" RH cases only as well as all time periods. "Low" RH is defined as less than 60%.

The growth and phase change of the particles, of course, affects their light scattering efficiency. In general, the higher the RH, the greater the scattering efficiency of sulfate and nitrate aerosols. The relationship between RH and sulfate scattering efficiency, referred to as $f_s(\text{RH})$, is parameterized by a curve shown in Figure 5.1 based on one published by Tang et al.¹² A similar curve for nitrates, also based on one from Tang et al.¹² and referred to as $f_n(\text{RH})$ is shown in the same figure. These curves, which are based on theoretical scattering efficiencies for aerosols of different size distributions have sharp discontinuities at 62% RH for nitrates and at 80% for sulfates. These are the deliquescence points for these species. However, since both ammonium nitrate and ammonium sulfate are hygroscopic at 30% RH^{9, 11, 12} and since the growth factor and light scattering efficiency for ambient aerosols has previously been observed to be rather smooth,^{9, 10} for WHITEX, Tang's curves were smoothed between the respective deliquescence points and 30% RH. Tang's results also show that the scattering efficiency of ammonium sulfate at low relative humidities is quite sensitive to the particle size distribution and can vary between approximately 1.4 and 3.5 m^2/g . Similarly,

Relative Scattering Efficiencies

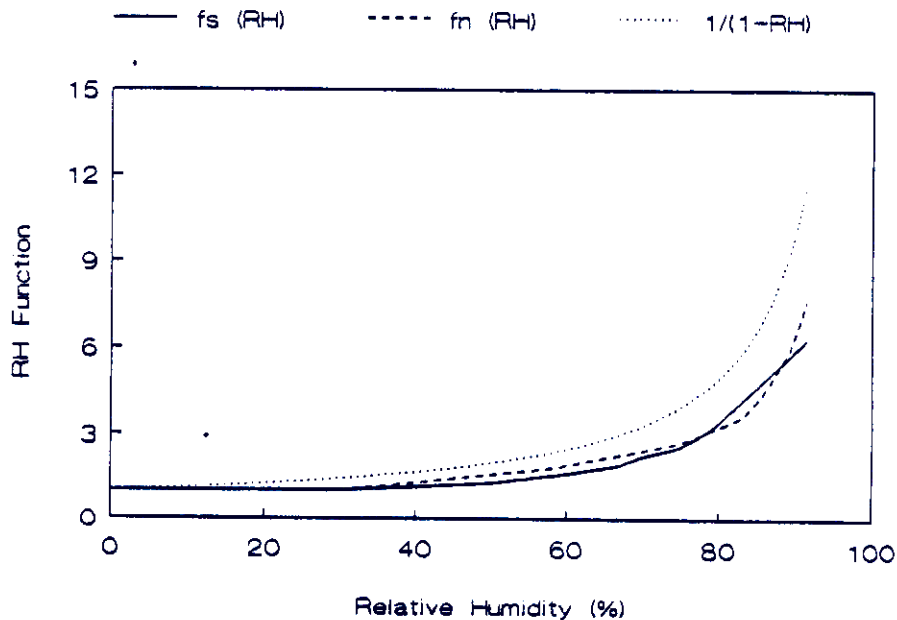


Figure 5.1: Relative light scattering coefficients for ammonium sulfate and ammonium nitrate aerosols.

the scattering efficiency of ammonium nitrate varies between approximately 1.1 and 7.0 m^2/g at low relative humidities depending on the size distribution.

For comparison, a curve showing $1/(1-RH)$ which has often been used in previous visibility studies¹³ is shown in the same figure. In the following analyses both $1/(1-RH)$ and the modified Tang curves will be used.

The nephelometers used in the WHITEX study dry the aerosols, thus reducing their scattering efficiency. Therefore the scattering coefficients measured by the nephelometers should be considered the "dry" scattering only. This is discussed further in the next section.

5.1.4 Multiple Linear Regression Analysis

One method of determining the scattering or absorbing efficiency of particulate matter is multiple linear regression (MLR). The dependent variable can be either the measured light extinction (b_{ext}) from the transmissometer or the measured light scattering (b_{scat}) from the nephelometer. The independent variables are the concentrations of particulate matter for each chemical species. The regression coefficients which result from such an analysis are estimates of the scattering or absorption efficiencies of the associated chemical species. When sulfates and nitrates are regressed against b_{ext} they are multiplied by the relative humidity function $f_s(RH)$ and $f_n(RH)$, respectively, as discussed above.

The WHITEX data analysis plan called for the use of structural regression which involves including explicitly the uncertainty of each variable into all multiple linear regression analyses. This was not possible since estimates of the uncertainties for most variables were not available until very recently. None of the analyses referred to in this chapter are structural regressions.

Collinearities between any two or more "independent" variables used in an MLR analysis would suggest that the variables were not in fact independent, leading to unstable regression coefficients with large standard errors. If the collinearities were very strong, then in addition to the large

Table 5.1: Pearson correlation coefficients for data at Page.

| | b_{ext} | sulfates $\times fs(RH)$ | nitrates $\times fn(RH)$ | organics | abs. C | fine soil | coarse mass | NO_2 |
|--------------------------|-----------|-----------------------------|-----------------------------|----------|--------|-----------|----------------|--------|
| b_{ext} | 1.000 | | | | | | | |
| sulfates $\times fs(RH)$ | 0.924 | 1.000 | | | | | | |
| nitrates $\times fn(RH)$ | 0.472 | 0.409 | 1.000 | | | | | |
| organics | 0.399 | 0.240 | 0.397 | 1.000 | | | | |
| abs. C | 0.396 | 0.268 | 0.627 | 0.695 | 1.000 | | | |
| fine soil | 0.193 | 0.108 | 0.524 | 0.231 | 0.416 | 1.000 | | |
| coarse mass | 0.030 | -0.122 | 0.178 | 0.113 | 0.309 | 0.458 | 1.000 | |
| NO_2 | 0.214 | 0.001 | 0.056 | -0.017 | 0.252 | 0.279 | 0.339 | 1.000 |

Table 5.2: Pearson correlation coefficients for Canyonlands.

| | b_{ext} | sulfates $\times fs(RH)$ | nitrates $\times fn(RH)$ | organics | abs. C | fine soil |
|--------------------------|-----------|-----------------------------|-----------------------------|----------|--------|-----------|
| b_{ext} | 1.000 | | | | | |
| sulfates $\times fs(RH)$ | 0.479 | 1.000 | | | | |
| nitrates $\times fn(RH)$ | 0.451 | 0.537 | 1.000 | | | |
| organics | 0.462 | 0.209 | 0.329 | 1.000 | | |
| abs. C | 0.402 | 0.009 | 0.234 | 0.599 | 1.000 | |
| fine soil | 0.036 | -0.063 | 0.169 | -0.008 | 0.059 | 1.000 |

standard errors, there would be numerical difficulty in inverting the matrix which would lead to regression coefficients which were inaccurate. To check for collinearities in the WHITEX data, the particulate concentrations at Page, Canyonlands, and Hopi Point were subjected to three diagnostic tests. The first was to generate a correlation matrix, second was a factor analysis followed by Varimax rotation, and third a collinearity test suggested by Belsley et al.¹

The correlation matrices for all the relevant data are shown in Tables 5.1, 5.2, 5.3, and 5.4. They show that at Page, nitrates are fairly highly correlated with both carbonaceous material and fine soil. At Canyonlands, humidity corrected sulfates and nitrates are somewhat correlated. As expected, light absorbing carbon correlates fairly well with organic carbon, and fine soil is somewhat correlated with coarse mass at all sites.

Although the correlation matrices suggest there may be some problems with collinearities, the two diagnostic tests based on eigenvector extraction do not. Varimax rotation forces each variable to load as strongly as possible onto a single factor, while loading lightly on all other factors. If collinearities exist, the collinear variables would load onto the same factor. Results of the factor analyses for the three sites are shown in Tables 5.5, 5.6, 5.7, and 5.8. Since none of the variables except organics and elemental carbon at Canyonlands loaded strongly together, the results suggest no collinearity problems.

The Belsley collinearity test shows the amount each eigenvector of the sums of cross products and squares data matrix contributes to the variance of each regression coefficient. If an eigenvector with a small eigenvalue contributes strongly to the variance of two or more components, then a

Table 5.3: Pearson correlation coefficients for data at Hopi Point.

| | b_{ext} | sulfates $\times fs(RH)$ | nitrates $\times fn(RH)$ | organics | abs. C | fine soil | coarse mass |
|--------------------------|-----------|-----------------------------|-----------------------------|----------|--------|-----------|----------------|
| b_{ext} | 1.000 | | | | | | |
| sulfates $\times fs(RH)$ | 0.711 | 1.000 | | | | | |
| nitrates | 0.718 | 0.467 | 1.000 | | | | |
| organics | 0.195 | 0.038 | 0.201 | 1.000 | | | |
| abs. C | 0.596 | 0.174 | 0.350 | 0.634 | 1.000 | | |
| fine soil | 0.315 | -0.025 | 0.185 | 0.191 | 0.090 | 1.000 | |
| coarse mass | 0.288 | -0.068 | 0.301 | 0.073 | 0.048 | 0.675 | 1.000 |

Table 5.4: Pearson correlation coefficients for Page, Canyonlands, and Hopi Point combined.

| | b_{ext} | sulfates $\times fs(RH)$ | nitrates $\times fn(RH)$ | organics | abs. C | fine soil | coarse mass |
|--------------------------|-----------|-----------------------------|-----------------------------|----------|--------|-----------|----------------|
| b_{ext} | 1.000 | | | | | | |
| sulfates $\times fs(RH)$ | 0.863 | 1.000 | | | | | |
| nitrates $\times fn(RH)$ | 0.557 | 0.464 | 1.000 | | | | |
| organics | 0.462 | 0.550 | 0.259 | 1.000 | | | |
| abs. C | 0.542 | 0.244 | 0.505 | 0.762 | 1.000 | | |
| fine soil | 0.125 | 0.037 | 0.266 | 0.145 | 0.236 | 1.000 | |
| coarse mass | 0.237 | -0.009 | 0.354 | 0.351 | 0.434 | 0.491 | 1.000 |

Table 5.5: Rotated factor pattern for Page.

| Variable | Factor 1 | Factor 2 | Factor 3 | Factor 4 | Factor 5 | Factor 6 |
|--------------------------|----------|----------|----------|----------|----------|----------|
| b_{ext} | 0.951 | 0.225 | 0.133 | 0.011 | 0.042 | 0.042 |
| sulfates $\times fs(RH)$ | 0.968 | 0.043 | 0.155 | -0.107 | 0.013 | 0.052 |
| nitrates $\times fn(RH)$ | 0.266 | 0.222 | 0.885 | 0.061 | 0.268 | 0.144 |
| organics | 0.184 | 0.954 | 0.172 | 0.039 | 0.105 | 0.112 |
| abs. carbon | 0.148 | 0.544 | 0.472 | 0.176 | 0.177 | 0.630 |
| fine soil | 0.031 | 0.121 | 0.230 | 0.229 | 0.935 | 0.073 |
| coarse mass | -0.081 | 0.056 | 0.061 | 0.970 | 0.204 | 0.062 |

Table 5.6: Rotated factor pattern for Canyonlands

| Variable | Factor 1 | Factor 2 | Factor 3 | Factor 4 | Factor 5 |
|--------------------------|----------|----------|----------|----------|----------|
| b_{ext} | 0.286 | 0.255 | 0.205 | -0.015 | 0.894 |
| sulfates \times fs(RH) | 0.092 | 0.921 | 0.177 | -0.005 | 0.216 |
| nitrates \times fn(RH) | 0.156 | 0.178 | 0.951 | 0.077 | 0.178 |
| organics | 0.787 | 0.475 | 0.093 | -0.069 | 0.096 |
| abs. carbon | 0.892 | -0.081 | 0.139 | 0.039 | 0.251 |
| fine soil | -0.005 | -0.012 | 0.066 | 0.997 | -0.010 |

Table 5.7: Rotated factor pattern for Hopi Point

| Variable | Factor 1 | Factor 2 | Factor 3 | Factor 4 | Factor 5 | Factor 6 |
|--------------------------|----------|----------|----------|----------|----------|----------|
| b_{ext} | 0.621 | 0.478 | 0.257 | -0.061 | 0.429 | 0.126 |
| sulfates \times fs(RH) | 0.957 | 0.115 | 0.030 | 0.110 | 0.182 | 0.015 |
| nitrates \times fn(RH) | 0.336 | 0.325 | 0.074 | 0.186 | 0.841 | 0.156 |
| organics | 0.076 | 0.183 | 0.075 | 0.962 | 0.114 | 0.081 |
| abs. carbon | 0.184 | 0.897 | 0.000 | 0.255 | 0.257 | 0.097 |
| fine soil | 0.093 | 0.023 | 0.926 | 0.085 | 0.070 | 0.334 |
| coarse mass | 0.044 | 0.107 | 0.355 | 0.092 | 0.133 | 0.914 |

Table 5.8: Rotated factor pattern for Page, Canyonlands, and Hopi Point combined.

| Variable | Factor 1 | Factor 2 | Factor 3 | Factor 4 | Factor 5 |
|--------------------------|----------|----------|----------|----------|----------|
| b_{ext} | 0.876 | 0.285 | 0.235 | 0.036 | 0.182 |
| sulfates \times fs(RH) | 0.959 | 0.096 | 0.143 | 0.023 | 0.081 |
| nitrates \times fn(RH) | 0.278 | 0.207 | 0.901 | 0.129 | 0.227 |
| organics | 0.260 | 0.894 | 0.200 | 0.054 | 0.297 |
| abs. carbon | 0.221 | 0.460 | 0.319 | 0.122 | 0.789 |
| fine soil | 0.030 | 0.048 | 0.099 | 0.991 | 0.071 |

Table 5.9: Consensus literature light extinction efficiencies in m^2/g .

| | Trijonis and Pitchford ¹³ | Used for WHITEX |
|------------------|--------------------------------------|-----------------|
| sulfates | 2.55/(1-RH) | 2.55 × fs(RH) |
| nitrates | same as sulfates | †1.1 × fn(RH) |
| organics | 3.75 | 4.0 |
| absorbing carbon | 9.0 | 9.0 |
| coarse mass | 0.6 | 0.45 |
| fine soil | 1.25 | 1.25 |

†This extinction efficiency was taken from Tang et al.¹² and is based on a mass median diameter of 0.98 μm and a highly polydisperse size distribution.

collinearity problem exists. The results of the Belsley test also showed no collinearity problems in the particulate data.

The three diagnostic tests indicate that collinearities in the WHITEX data are not strong enough to cause numerical difficulties with matrix inversion in the MLR analyses. However, they may be large enough to cause large standard errors in some regression coefficients. Standard errors for all regression coefficients will be reported in the following sections.

5.1.5 Consensus Scattering and Absorption Efficiencies

In some of the following analyses “consensus literature” scattering and absorption efficiencies for different chemical species are used. These values are based on a literature review by Trijonis and Pitchford.¹³ The values suggested by them in m^2/g are shown in Table 5.9 along with the values used for the WHITEX study. The scattering efficiency for organics which was suggested by Trijonis and Pitchford was scaled by 1.5/1.4 since they assumed that organics were $1.5 \times [organic\ C]$ while 1.4 was used as the mass multiplier for WHITEX. The coarse mass scattering efficiency suggested by Trijonis and Pitchford is for particles 2.5–10 μm in diameter. Since WHITEX coarse mass data are 2.5–15 μm , Trijonis¹⁴ suggested reducing the efficiency to 0.45 m^2/g for this data set. Best estimates for the scattering efficiencies of ammonium sulfate and ammonium nitrate are those given by Tang¹² for highly polydisperse particle size distributions, although reconstructed scattering was also calculated using the Trijonis and Pitchford¹³ efficiencies for these species.

5.1.6 Reconstructed Scattering and Extinction

Using either consensus literature or MLR derived scattering and absorption efficiencies, reconstructed scattering can be calculated by

$$\begin{aligned}
 b_{scat,R} &= E_S \times [sulfates] + E_N \times [nitrates] + E_{CT} \times [total\ C] \\
 &+ E_{FS} \times [soil] + E_{CM} \times [coarse\ mass]
 \end{aligned}
 \tag{5.7}$$

where E_S , E_N , E_{CT} , E_{FS} , and E_{CM} are the scattering efficiencies of sulfates, nitrates, total carbon, fine soil, and coarse mass. The scattering efficiency of total carbon is assumed to be the same as for organics alone.

Similarly, reconstructed extinction can be calculated by

$$b_{ext,R} = E_S \times [sulfates] + E_N \times [nitrates] +$$

$$E_{CT} \times [\text{organic } C] + E_{AC} \times [\text{abs. } C] + E_{FS} \times [\text{soil}] + E_{CM} \times [\text{coarse mass}] \quad (5.8)$$

The efficiencies are defined the same as those in Equation 5.7. E_{AC} is the absorption efficiency for light absorbing carbon.

5.2 Preliminary Data Analysis

Before attempting the estimation of light extinction efficiencies and budgets with WHITEX data, some preliminary analyses of the data were performed. These included (1) an investigation of extinction coefficients measured by the transmissometer compared to scattering coefficients measured by the integrating nephelometer for the full range of relative humidity conditions; and (2) comparisons of the results of several analyses using the extinction and scattering coefficients and particulate matter concentrations for separate carbon and nitrate data sets. These were used to examine whether use of light extinction data could help resolve the discrepancies between collocated measurements of carbon and nitrate and perhaps illuminate which data sets would be more appropriate to use in subsequent analyses, including estimation of extinction efficiencies and budgets. Refer to Chapter 3 for more discussion of the carbon and nitrate measurements.

5.2.1 Optical Data and Relative Humidity Effects

Historically, most short term and many long term visibility research programs have relied on the integrating nephelometer as the instrument of choice for measuring atmospheric aerosol scattering. Atmospheric extinction was then approximated by estimating the absorption coefficient. Atmospheric absorption is usually determined using the laser integrating plate method (LIPM) or by measuring elemental carbon and assuming a light absorption efficiency. Given the large discrepancies found in this and other studies between elemental carbon measurements and between elemental carbon derived absorption and LIPM, determinations of extinction by these methods are approximate at best.

Fortunately, Page, Canyonlands, and Hopi Point, were each equipped with both a nephelometer and a transmissometer, which measures extinction directly. This allowed intercomparison of the scattering coefficients measured by the nephelometer (b_{scat}) to the extinction coefficients measured by the transmissometer (b_{ext}). Relative humidity (RH) was also monitored at each of these sites. Time traces of these data, as well as the differences between b_{ext} and b_{scat} and the ratios of b_{ext}/b_{scat} are shown in Figures 5.2, 5.3, and 5.4. Note that the largest extinction coefficients occurring during WHITEX were measured at Page during Feb. 11 - 13 (Julian days 42 - 44) when the relative humidity remained above 60 percent for several days.

At Hopi Point and Canyonlands, transmissometer data are often missing when the relative humidity is high. This is a result of the altitudes of these sites (7100 and 5925 feet above mean sea level, respectively) which frequently causes the sight paths to be obscured by clouds on high RH days. The elevation at Page (4180 feet) is apparently low enough so that this did not occur as frequently.

Scatter plots of the ratios of b_{ext}/b_{scat} as a function of relative humidity are shown in Figures 5.5, 5.6, and 5.7 for the three sites. The mean ratios are near unity (1.10, 1.03, and 1.28 for Page, Hopi Point, and Canyonlands, respectively) when the relative humidity is below 60 percent. As discussed above, there are few transmissometer data at Hopi Point and Canyonlands when the relative humidity is higher than this. However, at Page, it can be seen that the ratio increases dramatically as the relative humidity increases from 70 to near 100 percent. It is known that